Comparing Batch Column Configurations: Parametric Study Involving Multiple Objectives

Ki-Joo Kim and Urmila M. Diwekar
Civil and Environmental Engineering, Environmental Institute, Carnegie Mellon University, Pittsburgh, PA 15213

The principal objective of this study is to advance the state of the art in batch distillation synthesis by providing insights into the behavior of various column configurations, including emerging column designs, using systematic parametric performance indices. Three competing column configurations—the rectifier, the stripper, and the middle vessel column—were compared in terms of various performance indices. Performance indices used include product purity and yield, design feasibility and flexibility, and thermodynamic efficiency. Product purity is related to profitability when yield is constant. Feasibility indices based on the number of plates and the reflux ratio show whether or not such a high-purity configuration is flexible for changing design and operating conditions. Thermodynamic efficiency provides a measure of effectiveness of heat exchange around the specific column configuration. Trade-offs between these performance indices are presented.

Introduction

The recent increase in the production of high value-added, low-volume specialty chemicals and biochemicals has generated renewed interest in batch processing technologies. Batch distillation is a widely used and important unit operation in the batch processing industry. The most outstanding feature of batch distillation is its flexibility in design and operation. It is this flexibility along with the unsteady-state nature of the process that poses challenging design and operation problems.

However, the conceptual design of batch distillation is difficult to obtain compared to continuous distillation synthesis, and is usually carried out using trial-and-error approaches and pilot plant studies. This is due to the two reasons: (1) the process is time-varying and one has to resort to complex numerical integration techniques and different models for obtaining the transients; and (2) this ever-changing process also provides flexibility in operating and configuring a column in numerous ways, some of which are shown in Figure 1. The column in Figure 1a is a conventional batch distillation column, or a rectifier. Figure 1b represents an inverted column for separating heavy ends as bottom products. It is often called a stripper, where the original feed mixture is charged into the top still pot. Although the inverted column was originally discussed by Robinson and Gilliland in 1950, it has gained its popularity in recent years. Davidyan et al. published a middle-vessel column in 1994. The middle-vessel column has both stripping and rectifying sections embedded in it (Figure 1c). It is known that this configuration provides added flexibility for batch distillation because of its new degree of freedom (q'), which is the ratio of the vapor flow rate in the top section to the vapor flow rate in the bottom section. It is also claimed that a recovery of 100% of pure components into the distillate, the middle-vessel residue, and the bottom product can be possible for the ternary system in the middle-vessel column (Safrit et al., 1995). Skogestad et al. (1997) reported a new column configuration called a multivessel column, as shown in Figure 1d, which is a generalization of the middle-vessel column at total reflux, and they showed that it can obtain pure products at the end of the operation for multicomponent systems. Hasebe et al. (1997) also studied a similar column configuration that is called the multieffect batch distillation system. These are a few examples of various batch distillation column designs. Combined with different possible operating modes and/or recycles, the number of column configuration tends to be very high, which poses a complex synthesis problem.

Correspondence concerning this article should be addressed to U. M. Diwekar.

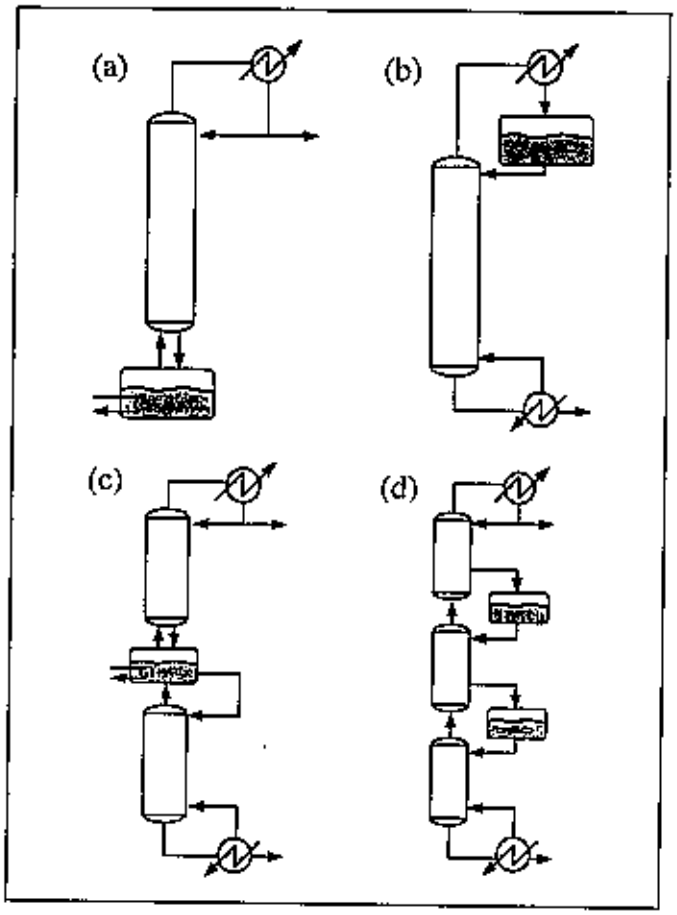

Figure 1. Example of different batch column configurations.

(a) Rectifier; (b) stripper; (c) middle-vessel column; and (d) multivessel column.

While the batch rectifier has a long history and is widely used in pharmaceutical and specialty chemical industries, the emerging columns have little implementation, partly due to the short history and limited knowledge of the behavior of these columns. In the earlier studies of comparing batch column configurations, performance indices such as product purity, batch time, or total cost were mainly used. Chiotti and Iribarren (1991) compared a rectifier with a stripper in terms of the annual cost and product purity. They concluded that the rectifier is better for more volatile component (MVC) products and that it is economical to obtain less volatile component (LVC) products using the stripper. But their annual cost analysis did not provide any heuristics because of their case-dependent observations and limited parametric studies. Hasebe et al. (1992) proposed a different result, in which a rectifier always has a higher separation efficiency than a stripper. Mujtaba and Macchietto (1994) discussed the application of a rectifier, a stripper, and a middle-vessel column to reactive batch distillation, which resulted in the lowest conversion in the stripper. Meski and Morari (1995) also compared the three column configurations in terms of optimal batch time under pure product purity, infinite separation, and minimum reflux assumptions. It is found that the middle-vessel column always has the shortest batch time for almost all feed compositions, and the rectifier has the next shortest time. Sørensen and Skogestad (1996) studied the performance and dynamic behavior of a rectifier and a stripper in terms of minimum optimal operating time. They concluded that the stripper is the preferred column configuration when a small amount of light key is in the feed and that the rectifier is better when the feed has a high amount of the light key. Although a number of studies support the same heuristics, there are also studies that present contradictions between the proposed heuristics. For instance, the effect of batch time with respect to feed composition presented by Meski and Morari (1995) and Sørensen and Skogestad (1996) conflict with each other. This can be partly due to the limited ranges of parameters and chemical systems considered. Further, the parameters or performance indices used in the earlier studies represent only some of the attributes of the batch distillation design process in real practice, and hence additional parameters are required for more comprehensive column comparisons. For example, the flexibility of batch distillation is one major attribute for design, and thus the same column can be used for different feed stocks. This calls for consideration of a feasibility window at the early design stage. Another important factor for column selection can be the optimal heat-exchange configuration for emerging columns that are not widely implemented in real practice. Consideration of the optimal heat-exchange configuration, such as where heat needs to be added or to be rejected, is going to be a major issue in making these columns widely accepted in the real world. Here, we evaluate the thermodynamic efficiency as a measure for the effectiveness of heat exchange around the specific column configuration. In this study we define and quantify the additional objectives such as feasibility indices and thermodynamic efficiency. To obtain general heuristics and trade-offs, a systematic parametric approach and a multiobjective framework is presented here.

The principal objective of the study is to advance the state of the art in batch distillation synthesis by providing insights into the behavior of the various column configurations and emerging designs of batch distillation using systematic parametric approaches. Three competing columns, such as the rectifier, the stripper, and the middle-vessel column, are compared in accordance with the multiple performance indices. The performance indices used are product purity and yield, design feasibility and flexibility, and thermodynamic efficiency. The systematic parametric studies and additional performance indices provide robust and generalized heuristics and present useful trade-offs for the designers.

This article is organized as follows: the following section briefly describes the design of experiments for systematic parametric studies. Definitions and derivations of performance indices are presented in the third section. The fourth section deals with results and discussions, and the last section elicits conclusions and suggestions for further work on the synthesis of optimal batch-column configuration.

Design of Experiments

In order to elicit generalized heuristics for batch column comparisons, this article evaluates four performance indices under wide ranges of design and operating conditions. Instead of exhaustive experiments or sensitivity studies, the systematic design of experiments based on a statistical sampling

Table 1. Ranges of Design and Operating Variables for Design of Experiments

Variable	Range
Feed A charge (kmol)	10 ~ 90
Feed B charge (kmol)	10 ~ 90
Vapor rate (kmol/h)	Same as feed charge
Relative volatility (α)	1.2 ~ 6.0
Reflux ratio (R)	1 ~ 10
Number of plates (N)	5 ~ 15
Number of samples	200

technique can represent the entire system with a smaller number of runs. A novel sampling technique, Hammersley sequence sampling (HSS) technique by Diwekar and Kalagnanam (1997), is used here for the design of experiments. This sampling technique can generate samples over the entire region more uniformly. Thus the HSS technique, which is established to be 3 to 100 times faster than the Latin hypercube sampling (LHS) and Monte Carlo sampling (MCS) techniques is a good technique for designing experiments.

All variables in Table 1 are allowed to span wide ranges of real batch distillation operation regimes in order to consider all possible cases. The vapor flow rate is set to the flow-rate equivalent to the amount of feed initially charged. For the middle-vessel column, the top vapor flow rate (V_T) is fixed similarly and the bottom vapor flow rate (V_B) is calculated from V_T and q'. Currently q' is not included in this table, as this parameter affects only the middle-vessel column. In the subsequent runs, q' is varied outside these experiment designs. The total number of plates for each column is set equal to be the same for identical experimental conditions. For the middle-vessel column, therefore, the number of plates in the top section (N_T) and in the bottom section (N_B) are the same, and the total number of plates ($N_T + N_B$) is, of course, equal to that of the rectifier or the stripper. When the total number of plates is an odd number, N_T is rounded up.

A comprehensive multibatch-distillation simulation package, MultiBatch*DS* (Diwekar, 1996), is used to evaluate the performance of the three-batch column configurations. Since the main purpose of this study is to obtain generalized heuristics for column configurations, we assumed an ideal binary system, constant molar overflow, constant relative volatility, and zero dry holdup for the batch column model in MultiBatch*DS*. At this stage, we restricted ourselves to constant reflux and constant reboil ratio operation policies, but we will consider different operation policies in the future.

Defining Objectives

As stated earlier, comprehensive heuristics for optimal column configuration cannot be obtained by limited studies in parameters, systems, or objectives. This section therefore briefly discusses the multiple performance indices used in this study: product purity and yield, feasibility, and thermodynamic efficiency. These indices are related to profitability, flexibility, and optimal heat-exchange configuration, respectively. New indices for flexibility are introduced, and derivation of the thermodynamic efficiency of the three competing column configurations is also presented.

Product purity and yield

Since product purity is one of main concerns in batch distillation, it is always included in column comparison studies. As described earlier, Chiotti and Iribarren (1991) and Hasebe et al. (1992) chose product purity as a column comparison index. Instead, Meski and Morari (1995) and Sørensen and Skogestad (1996) used fixed product purity in order to find optimal batch time. In this study we compared batch columns using product purity under fixed batch time, and hence fixed product yield. More precisely, we define two product purity terms that are product purities of the MVC and the LVC, respectively.

Product yield here is defined as the amount of product collected in the accumulator, and the yield of the rectifier and the stripper are given by D and B, respectively:

$$D = \int_0^T \frac{V}{R+1} dt \qquad \text{for the MVC} \tag{1}$$

$$B = \int_0^T \frac{V_B}{R_B} dt \qquad \text{for the LVC.} \tag{2}$$

For each experiment design, to keep the yield constant, the vapor flow rate, reflux ratio, and batch time are fixed, and V_B is set equal to V and R_B is equal to $R+1$. For the middle-vessel column, the product yields in the top and bottom sections are similarly defined as D and B in the preceding equations.

We can analyze batch column configurations in terms of product purity with fixed batch time and product yield. Under these conditions product purity is directly proportional to profitability or economic benefit of the column configuration.

Feasibility indices

The most outstanding feature of batch distillation is its flexibility. This flexibility allows one to deal with uncertainities in feed stock or product specification. Also one can handle several mixtures just by switching the column's operating conditions, a simple procedure. Therefore, feasibility study in batch distillation is central for design, optimization, and control of batch columns.

Feasibility is closely related to flexibility. In the literature, flexibility is quantified in terms of the flexibility index defined by Swaney and Grossmann (1985). The geometric definition of the flexibility index is the maximum rectangle possible in a *feasible* space, and it can be rewritten as the maximum amount of deviation a design can tolerate. Obviously the bigger the feasible region, the higher the flexibility and the feasibility index.

To obtain this operational flexibility, appropriate constraints are to be imposed on the variables, especially for such design variables as the number of plates (N or N_B) and the reflux ratio (R) or reboil ratio (R_B). Individual feasibility limits for the rectifier, the stripper, and the middle-vessel column were provided by Diwekar and Madhavan (1991) and Lotter and Diwekar (1997) by using the shortcut model. Here we define new feasibility indices in terms of the number of plates and the reflux (reboil) ratio. At the constant reflux or

constant reboil policy, the *instantaneous* N_{min} can be calculated from the modified Fenske equation for batch distillation, and the instantaneous N_{min} is averaged over the batch time. Thus the feasibility of the batch column in terms of N-feasibility index is given by

$$N\text{-feasibility index} = 1 - \frac{(N_{min})_{avg}}{N} \quad \text{for a rectifier}$$

$$= 1 - \frac{(N_{B,min})_{avg}}{N_B} \quad \text{for a stripper.} \quad (3)$$

For the middle-vessel column, the preceding equations can be used to evaluate the N-feasibility index for the top and bottom sections, respectively. The N-feasibility index can vary from 0 to 1 since N_{min} is less than the number of plates. An N-feasibility index that is closer to 1 is equivalent to saying that the design can tolerate more changes in design and operating conditions (better flexibility) and vice versa.

Like the number of plates, the reflux ratio (reboil ratio) also has a lower bound that is the minimum reflux ratio (R_{min}) or the minimum reboil ratio ($R_{B,min}$). This Underwood R_{min} corresponds to the reflux ratio at an infinite number of plates and provides a conservative lower bound for batch distillation. For the constant reflux conditions, however, the initial value of R has an actual lower bound, defined by the specified average distillate composition of the MVC of the rectifier. The initial distillate composition of the MVC is highest at the beginning and decreases as distillation progresses. If the initial value of R is such that the distillate composition of the MVC is less than the specified average, then it is impossible to meet the goal of attaining the specified average purity for the given number of plates. This criterion provides the lower limit, R_{MIN} on the initial R, in which R_{MIN} is defined as the value of R required to obtain the distillate composition of the MVC that is equal to the specified average distillate composition at the initial conditions for the given N. The possible range of R_{MIN}/R is (nearly) zero to infinity. An R_{MIN} greater than R means that the given distillation condition cannot meet the specified product purity, and thus R should be increased to be greater than R_{MIN}. An $R_{B,MIN}$ for the stripper can be calculated in a similar way. Therefore, the R-feasibility index can be defined as

$$R\text{-feasibility index} = 1 - \frac{R_{MIN}}{R} \quad \text{for a rectifier}$$

$$= 1 - \frac{R_{B,MIN}}{R_B} \quad \text{for a stripper.} \quad (4)$$

The maximum value of the R-feasibility index is 1 due to the range of R_{MIN}/R. When it goes to 1, the feed mixture can be easily separated at a reasonable reflux ratio (reboil ratio). In contrast to the N-feasibility index, the R-feasibility index can be negative if the specified average product purity is higher than the actual calculated average product purity.

Feasibility indices defined in terms of N and R shows how close the column configuration is to the limiting performance.

Thermodynamic efficiency

Thermodynamic efficiency (η) indicates how close a process is to its ultimate performance and also suggests whether or not the process can be improved. Thermodynamic efficiency is different from the first efficiency law or the Carnot engine efficiency. The first efficiency law deals with the ratio of heat transferred to heat supplied, and hence does not consider any energy quality, energy degradation, or equipment involved. Thermodynamic efficiency, however, can handle energy quality and energy degradation with or without work production during the process. Thus, it can be used as a column performance index to decide how the heat exchange can be improved around the specific column configuration.

Exergy analysis is required to evaluate thermodynamic efficiency. Exergy (ϵ, J/mol) is the maximum work attainable from a process stream to its reference state during a reversible process. Because all natural processes are not reversible, there is always exergy loss. Exergy is a thermodynamic state function and is defined as $h - T_o s$, which is derived from the difference between the first and second thermodynamic laws.

Exergy analysis has been conducted to reveal how efficient continuous distillation columns are, especially for cryogenic distillation, which demands large amounts of energy. Fitzmorris and Mah (1980) defined four different thermodynamic efficiency equations for several ethylene–ethane distillation column configurations and discussed strategies to improve distillation process in terms of thermodynamic efficiency. Agrawal and Herron (1997, 1998) identified optimal thermodynamic feed conditions for ideal binary distillation systems in terms of η, and extended their work to the analysis of the impact of an intermediate reboiler or condenser on binary distillation systems. Agrawal and Fidkowski (1998) compared thermodynamic efficiency of various ternary distillation configurations such as a side-rectifier, a side-stripper, and a fully coupled configuration. Unlike the earlier researchers, they found that for the fully coupled configuration, which has been known to have the lowest energy demand, this heuristic is only obtained in limited ranges in the feed composition and relative volatilities. Therefore, thermodynamic efficiency seems to be a useful performance index. The following definition of thermodynamic efficiency is used in literature:

$$\eta = \frac{W_{min}}{W_{min} + \epsilon_{loss}}, \quad (5)$$

where

$$W_{min} = \Sigma \epsilon_{out}^{mixing} - \Sigma \epsilon_{in}^{mixing} \quad (6)$$

$$\epsilon_{loss} = \Sigma \epsilon_{in} - \Sigma \epsilon_{out}. \quad (7)$$

The numerator, W_{min}, represents the minimum work of separation needed to get the specified product purity from the feed condition and can be evaluated by the chemical component (that is, mixing effects) of exergy. If the product purity is very high, then the W_{min} in continuous distillation is given by

$$W_{min} = -RT_o \Sigma x_{F,i} \ln x_{F,i}. \quad (8)$$

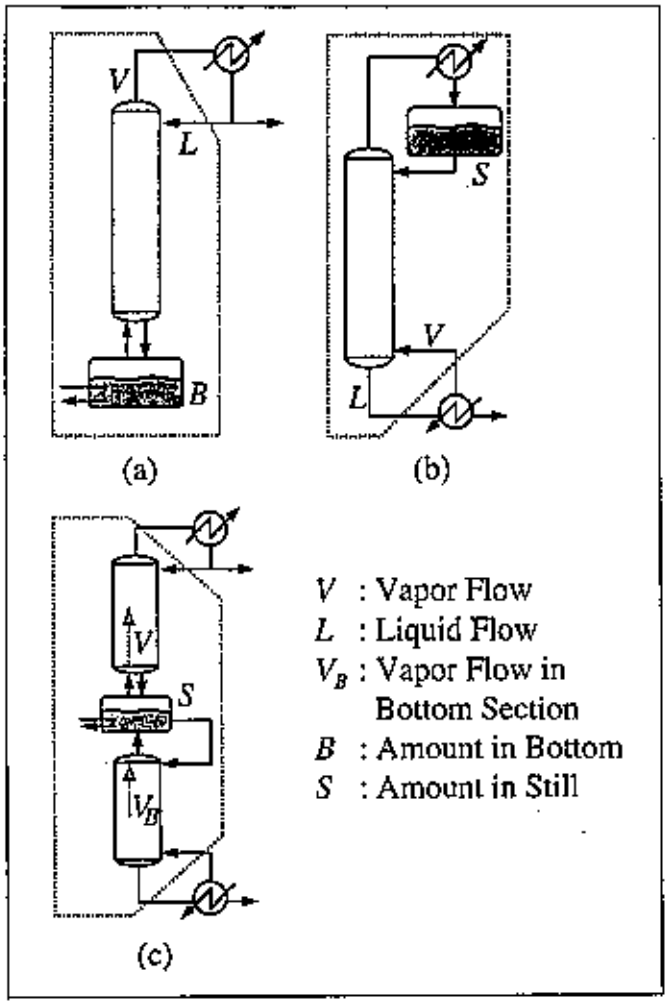

Figure 2. System boundaries for the exergy balance.
(a) Rectifier; (b) stripper; and (c) middle-vessel column.

And the denominator in Eq. 5 is the total exergy supplied for the desired separation and can be expressed as the summation of the minimum work and exergy loss during the process.

Thermodynamic efficiency of batch distillation is more complicated because of the unsteady-state nature of batch distillation. The system boundaries for exergy analysis in batch distillation are shown in Figure 2. In contrast to continuous distillation the reboiler in the rectifier, the top still pot in the stripper, and the middle vessel in the middle-vessel column are included in the system boundary. The reason is that these reservoirs can undergo large exergy changes during batch operation, and hence they will lower thermodynamic efficiency. This article presents the first exergy analysis for different batch column configurations. The following equations provide the expressions of η for various batch column configurations. Detailed derivation of the equations is presented in the Appendix.

For the rectifier, thermodynamic efficiency is derived as in the following equation:

$$\eta_{\text{rectifier}} = \frac{W_{\min}}{V \ln\left[\dfrac{x_{D,1}(\alpha-1)+1}{x_{B,1}(\alpha-1)+1}\right]}, \tag{9}$$

where

$$W_{\min}|_t = D\Sigma x_{D,i} \ln x_{D,i} - D\Sigma x_{B,i} \ln x_{B,i} + B\frac{d}{dt}(\Sigma x_{B,i} \ln x_{B,i}). \tag{10}$$

The $W_{\min}$ represents instantaneous minimum work. The first term in the $W_{\min}$ is the outgoing exergy by distillate, and the second and third terms represent exergy change in the reboiler. The last term is treated as a difference equation between the current and previous time steps. It can be seen that the thermodynamic efficiency of the rectifier is a function of the vapor flow rate, distillate rate, amount of bottom residue, distillate and bottom compositions, and relative volatility. The reboiler and condenser temperatures are not explicitly expressed in the equation like that of continuous distillation.

The thermodynamic efficiency for the stripper and the middle-vessel column are similarly derived and given by the following equations:

$$\eta_{\text{stripper}} = \frac{W_{\min}}{W_B \ln\left[\dfrac{x_{S,1}(\alpha-1)+1}{x_{B,1}(\alpha-1)+1}\right]} \tag{11}$$

$$\eta_{\text{middle}} = \frac{W_{\min}}{q'V_B \ln\left[\dfrac{X_{D,1}(\alpha-1)+1}{X_{S,1}(\alpha-1)+1}\right] + V_B \ln\left[\dfrac{X_{S,1}(\alpha-1)+1}{X_{B,1}(\alpha-1)+1}\right]}. \tag{12}$$

Note that the $W_{\min}$ equations for each column are different, and they are given in the Appendix. The stripper thermodynamic efficiency equation is similar to that of the rectifier. However, thermodynamic efficiency for the middle-vessel column has one additional variable (q'), which is the ratio of vapor flow rates between the top and the bottom sections. As stated earlier, batch column thermodynamic efficiencies are time dependent. Here we are using average values of thermodynamic efficiencies.

Results and Discussions

Design of experiments

This section analyzes the results of 200 experiments over the parametric window defined in Table 1 for three batch column configurations. The design of the experiments for the three columns was simultaneously conducted, and 600 data points per each performance index were analyzed for most cases. Using the multidimensional sampling by the HSS technique, we ensure that these runs provide the whole design and operating regions for batch-column comparison.

Product purity and yield

The performance index of product purity and yield is first analyzed for optimal column configuration. Two types of product purities, MVC and LVC, are compared under the

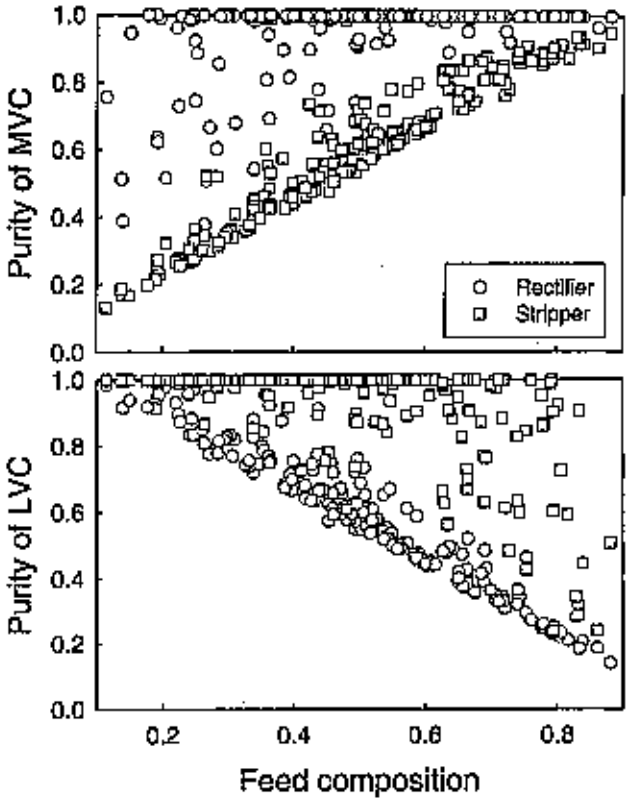

Figure 3. Comparison of batch columns in terms of product purity.

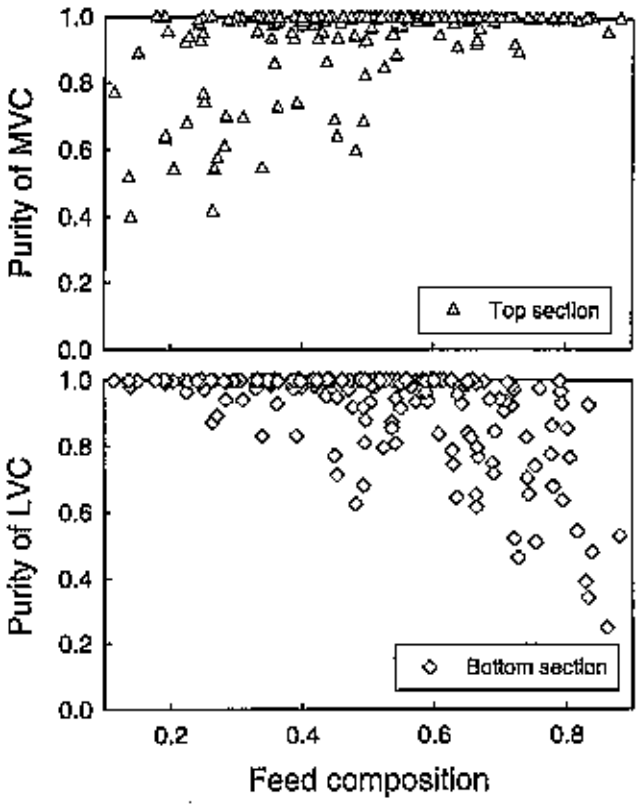

Figure 4. Product purity of the middle-vessel column.

same product yield. Figures 3 and 4 show the MVC and LVC product purities of the rectifier, the stripper, and the middle-vessel column in terms of feed composition. If higher purity of the MVC is desired, one should select the rectifier as the best column configuration regardless of design and operating conditions such as the reflux ratio, number of plates, and relative volatility, as well as feed composition. This preference for the rectifier (large product purity difference) is increased as the feed composition decreases. In contrast, it is found that the stripper is a promising column configuration for higher product purity of the LVC. Chiotti and Iribarren (1991) and Sørensen and Skogestad (1996) have shown similar findings. However, their results were not based on wide ranges of parametric studies and they did not present the preference direction in terms of product purity.

The middle-vessel column consists of a rectifier and a stripper both connected by the reservoir in the middle of the column, and its behavior becomes less predictable than a conventional batch column and has not been thoroughly studied. The parameter, q' in the middle vessel can significantly affect column dynamics in the top and bottom sections. In this article the product purity of the middle-vessel column with respect to q' is compared with those of the rectifier and the stripper. Figure 4 shows the product purity of the MVC and LVC of the middle-vessel column at q' of 1. For the top MVC product, the middle-vessel column shows similar performance to that of the rectifier, while for the LVC product, its behavior is close to that of the stripper. This means that the middle-vessel column can be an alternative of the rectifier and the stripper. Studying the effect of q' is helpful for providing insights into the behavior of the middle-vessel column. Figure 5 shows the product purity change with respect to q' at certain fixed conditions. The product purity of the MVC of the middle-vessel column is higher or almost the same as the rectifier purity at low q'. The MVC purity of the middle-vessel column decreases slightly, and eventually remains constant with increasing q'. Similar trends can be identified for the LVC product purity, but the purity difference between the middle-vessel column and the stripper becomes larger as q' increases. Thus, one can tune product purity by varying q' to achieve higher column performance, and this advantage can entitle the middle-vessel column with a flexible column configuration.

Although the general heuristics from product purity analysis hold good for most of the cases, as seen in Figures 3, 4, and 5, there are regions where the behavior of the three columns are so similar that it is hard to select one column configuration over the others. One thus needs another performance index or indices to get more insights for column comparison. As mentioned before, feasibility and thermodynamic efficiency can be used here, since they represent flexibility and optimal heat-exchange configuration around the batch columns. The following two sections deal with feasibility analysis, which shows how flexible the configuration is at the given condition, and thermodynamic efficiency, which shows how thermally efficient the chosen column is.

Feasibility indices

As stated earlier, there are two feasibility indices that are N-feasibility and R-feasibility indices. The minimum number

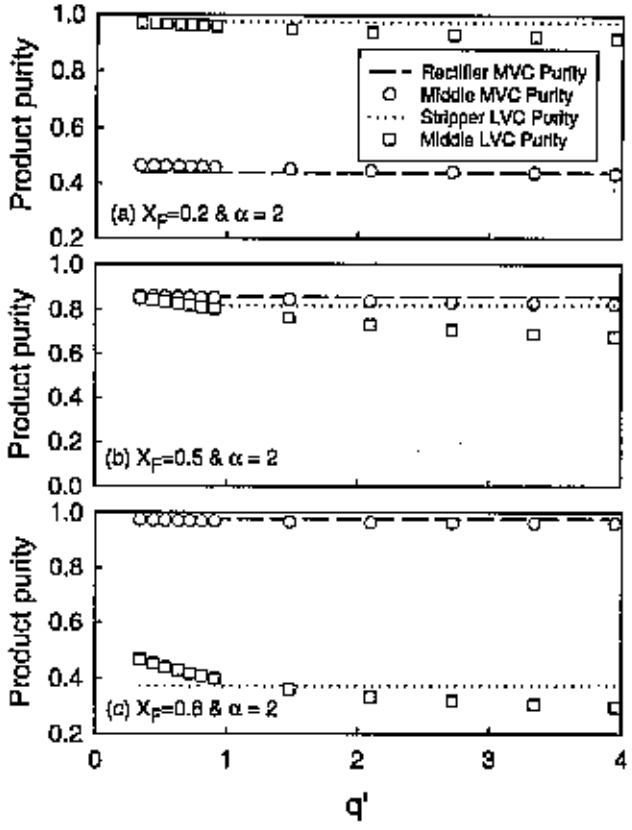

Figure 5. Effect of q' on the product purity of the middle-vessel column ($N = 5$ and $R = 2$).

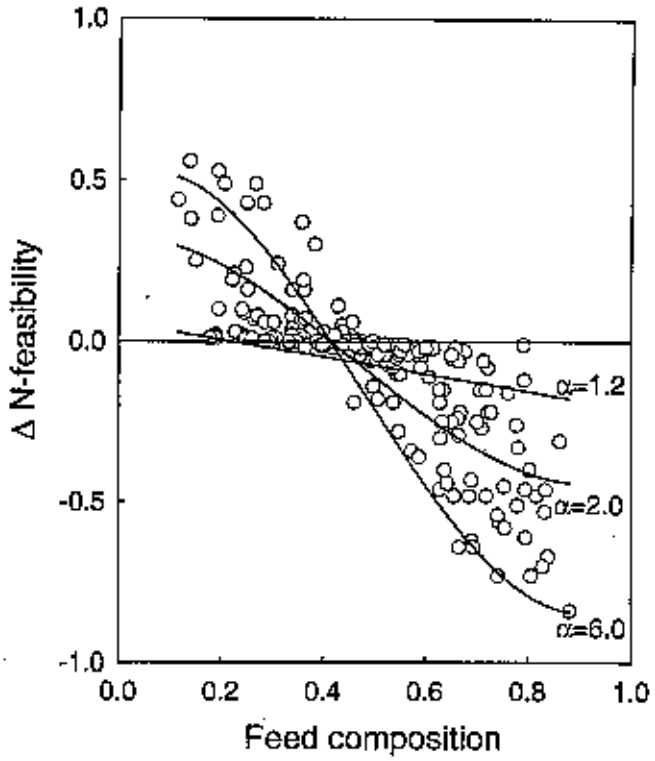

Figure 6. Effect of N-feasibility difference on the rectifier and the stripper.

of plates (N_{min} or $N_{B,min}$) for N-feasibility analysis is estimated by the modified Fenske equation for batch distillation. Because the N_{min} ($N_{B,min}$) is time dependent and generally decreasing as batch distillation proceeds, the N_{min} ($N_{B,min}$) at the average condition is used to evaluate the N-feasibility index. Because the *N-feasibility index* is bounded between 0 and 1 and has a distinctive superior region for each column, we defined the *Δ N-feasibility index* for the rectifier and the stripper, and the following term is used for N-feasibility analysis:

$$\Delta N\text{-feasibility index} = \left(1 - \frac{N_{min}}{N}\right) - \left(1 - \frac{N_{B,min}}{N}\right) = \frac{1}{N}(N_{B,min} - N_{min}). \quad (13)$$

Figure 6 shows the Δ N-feasibility index in terms of feed composition. A positive Δ feasibility index at low feed composition indicates higher rectifier N-feasibility, and a negative Δ feasibility index at high feed composition means better stripper N-feasibility. Since the stripper is not the true inversion of the rectifier, the feasibility difference is asymmetric. Solid lines in this figure show the N-feasibility difference at fixed conditions ($N = 5$ and $R = 2$). As α increases, it is observed that the N-feasibility difference increases due to improved product purity. From this observation it is said that the rectifier and the stripper have their distinctive regions, which can be a useful guideline for optimal column selection.

Similar trends for the middle vessel column can also be obtained.

Further valuable information can be obtained when the two performance indices, product purity and N-feasibility index, are considered together. As seen in the product purity section, the rectifier at low feed composition and the stripper at high feed composition can attain high product purity, and the N-feasibility study gives high flexibility to the columns at these conditions. However, considering multiple performance indices together is especially useful when one performance index cannot determine the best column configuration. For example, at high feed composition, the rectifier is still a promising column configuration in terms of the MVC purity, but the product purity of the stripper can also be comparable or equal to that of the rectifier. In this design situation, column comparison based on product purity would fail to give the best solution. The N-feasibility index of the stripper at this condition is much higher than that of the rectifier; this means that the stripper requires a small number of plates to attain the same product purity, and the number of stages may be reduced from the initial design stages. Thus at this condition it would be better for one to select the stripper as an optimal batch column configuration. Similarly, an opposite heuristic as an optimal column configuration can also be elicited at low feed compositions.

Like the N-feasibility index, there is also an R-feasibility index based on the reflux ratio or reboil ratio. How closely the given design can achieve the specified product purity is denoted by R_{MIN} ($R_{B,MIN}$). In order to evaluate R_{MIN}, the Underwood R_{min} and the Fenske N_{min} are obtained by equating the top composition at the initial condition to the

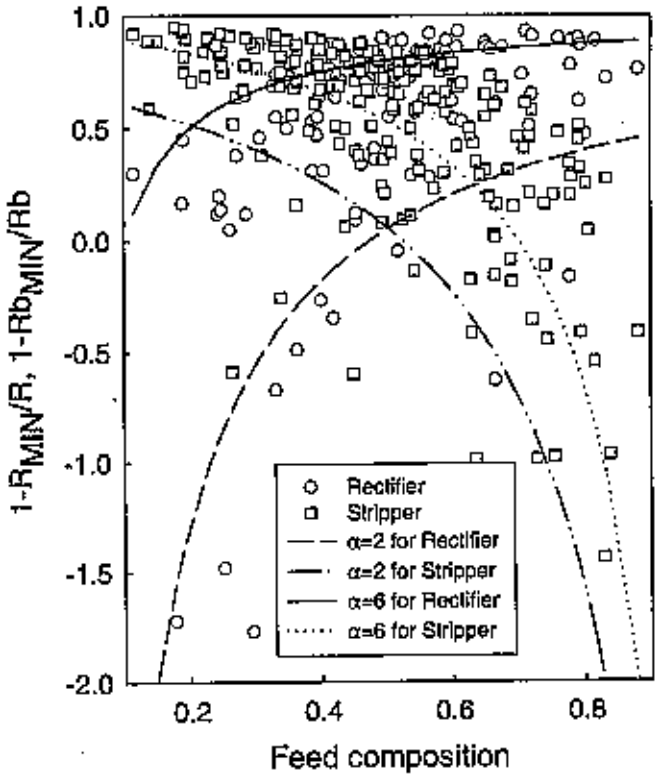

Figure 7. *R*-Feasibilities of the rectifier and the stripper [for clarity solid lines at fixed conditions (N = 5, R = 2) are added].

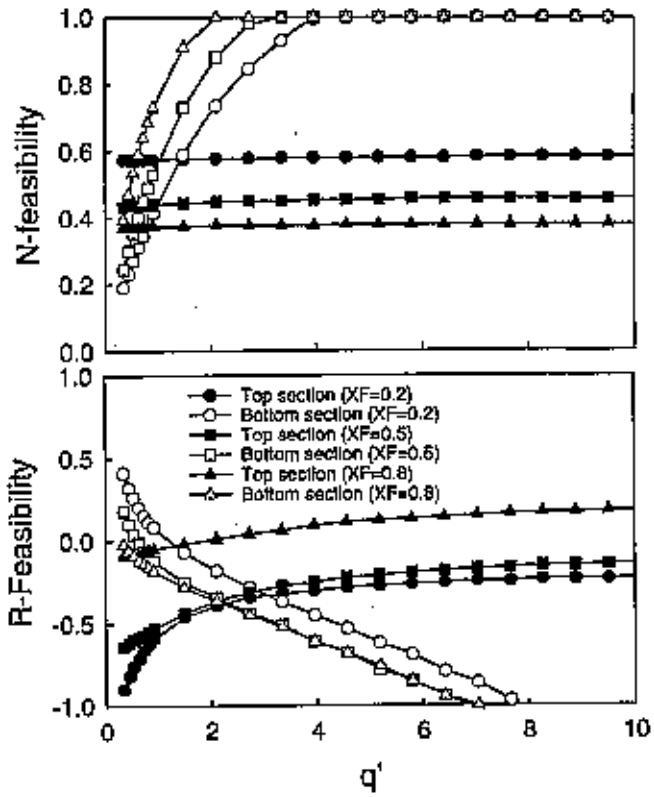

Figure 8. *N*- and *R*-feasibilities of the middle-vessel column with respect to q'.

specified average composition, and then R is calculated by using the Gilliland correlation. It should be remembered that this R, which is equal to R_{MIN}, is different from the Underwood R_{min}. The $R_{B,MIN}$ for the stripper and the middle-vessel column can be similarly calculated. If the initial product composition is less than the specified average product composition, then R_{MIN} ($R_{B,MIN}$) is greater than the given R (R_B), and the resulting R-feasibility defined in Eq. 4 becomes negative.

Figure 7 shows the R-feasibility index of the rectifier and the stripper, respectively. It is difficult to identify any trend for the R-feasibility index from this figure. This can be attributed to the fact that the R-feasibility index depends on α and N as well as feed composition. Even though the general trends in this figure are not as clear as that of the Δ N-feasibility index in terms of feed composition, in general it can be seen that the rectifier R-feasibility index increases with feed composition and the stripper R-feasibility index decreases with it. Most of the feasibility data are greater than 0.5, and several values are less than zero. These negative values correspond to low product purity at the given batch distillation condition and can be overcome by increasing the reflux ratio or reboil ratio. The general heuristics are to adjust N and R to obtain a good feasible design. Lines of different relative volatilities are also added in this figure for the simple idea of R-feasibility analysis. Like the effect of relative volatility on N-feasibility index analysis (Figure 6), relative volatility can also enhance the R-feasibility index, since product purity is improved, as relative volatility is increased as expected.

The added degree of freedom of the middle-vessel column, q', can also affect N- and R-feasibility indices. When q' is fixed at 1, it is observed that N- and R-feasibility of the middle-vessel column have similar trends as that of the rectifier or the stripper. Figure 8 shows the effect of q' on feasibility at fixed conditions. The N-feasibility index in the top section decreases very slowly and seems to be almost constant, while the N-feasibility index in the bottom section increases with q' and reaches up to 1. This is due to relatively low composition of the key component in the middle vessel. For the top section, the N-feasibility index, as q' increases, the top and middle-vessel product purities decrease together making the N-feasibility index constant. However, as the bottom product purity is decreasing with q', the resulting N-feasibility index increases.

The effect of feed composition is similar to the results shown in Figure 6. The effect of q' on the R-feasibility index is also shown in Figure 8. At the top section, the R-feasibility index increases with q', and at high values of q', the R-feasibility index is almost constant. This is due to the small change in the top product purity. Negative values are also found at highly specified product purity (say, x_D is 0.99). The bottom-section R-feasibility index is highly dependent on q', because the bottom product purity decreases as q' increases.

Thermodynamic efficiency

The last performance index used in this study is thermodynamic efficiency, which is a measure of the effectiveness of heat exchange around the specific column configuration. The

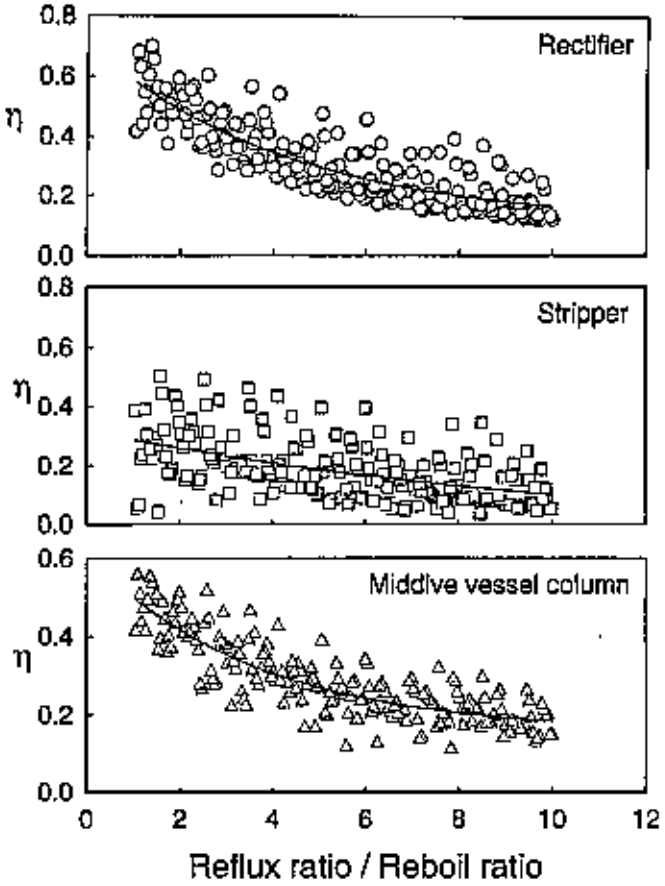

Figure 9. Effect of the reflux ratio on thermodynamic efficiency.

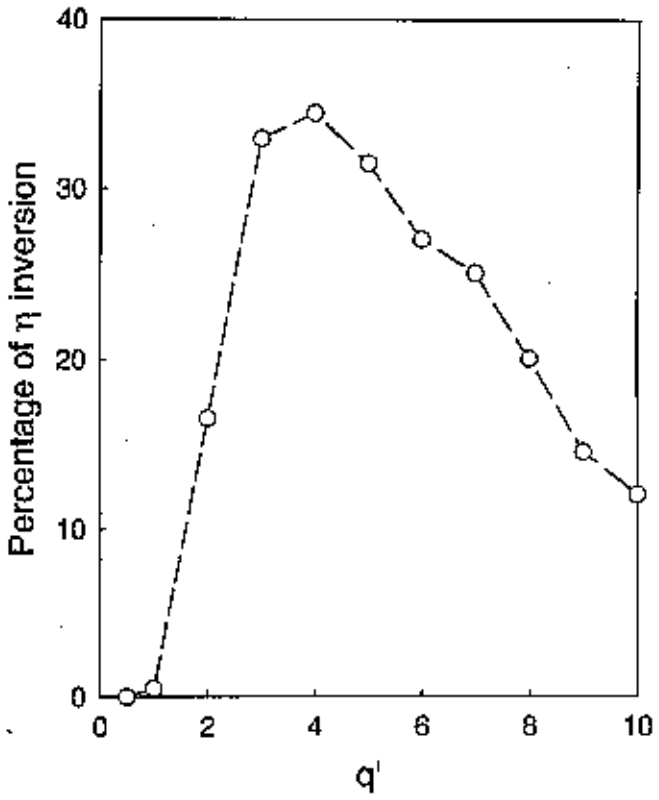

Figure 10. Percentages of thermodynamic efficiency inversion in the middle-vessel column.

thermodynamic efficiency equation derived here is a complex function of the vapor flow rate, the production rate, the amount in the reservoir, relative volatility, and compositions. Thus it is difficult to get simple heuristics from graphical representations just in terms of feed composition, as presented earlier. The effect of the reflux ratio on thermodynamic efficiency has a meaningful and expected trend from this experiment design, as shown in Figure 9. As R (R_B) increases, the increased product purity causes a decrease in the W_{min} equations and an increase in the denominator in the thermodynamic efficiency equations. Thus the resulting thermodynamic efficiency decreases with R (R_B) (that is, with increasing product purity).

It is observed that the thermodynamic efficiency of the rectifier is generally superior to that of the stripper or the middle-vessel column. Among 200 experiment design cases, the percentage that the stripper or the middle-vessel column has higher η is less than 4%. Thus one can expect that the thermodynamic efficiency inversion of the two columns is restricted to small regions of batch-distillation space, which needs to be explored. The generally superior efficiency of the rectifier can be ascribed to the inherent difference in the exergy balance. The required heat duty for the rectifier and stripper (Q_R and Q_S) can be assumed to be almost the same. However, in the stripper a hot stream of the bottom product is withdrawn from the system boundary and there is a composition difference between the liquid composition at tray N from the top (x_N) and the vapor composition at the reboiler (y_B), whereas a relatively cold distillate stream comes from the rectifier system boundary and the top steam has the same composition (x_D and y_D). The thermodynamic efficiency of the middle-vessel column can be explained in a similar way.

The additional degree of freedom in the middle-vessel column (q') can also exert a large impact on thermodynamic efficiency. As seen in Figure 10, the percentages of the η inversion defined as the fraction of the design cases of the middle vessel column that showed higher η than the rectifier, varies drastically with respect to q'. For example, if q' is 0.5, the inversion may not be statistically observed. As q' increases, the inversion percentages reach a maximum value at a certain value of q'. In this experiment design, at q' of 4 the middle-vessel column has a 34.5% chance of having a higher thermodynamic efficiency than that of the rectifier. Most of the inversion occurs at high product purity conditions. As described earlier, it is found that q' has a slight negative effect on product purity and the top section N-feasibility of the middle-vessel column, and thus the value of q' to increase thermodynamic efficiency should be optimized. This figure supports the idea that q' can be an important factor on thermodynamic efficiency of the middle-vessel column.

In order to elicit additional information from the thermodynamic efficiency index, the efficiency can be compared at certain fixed conditions because of its complexity. The complexity mainly comes from the strong dependency on the relative volatility and the reflux ratio. Figure 11 shows the typical efficiency trends of the three batch columns with respect to α and R. A higher thermodynamic efficiency of the recti-

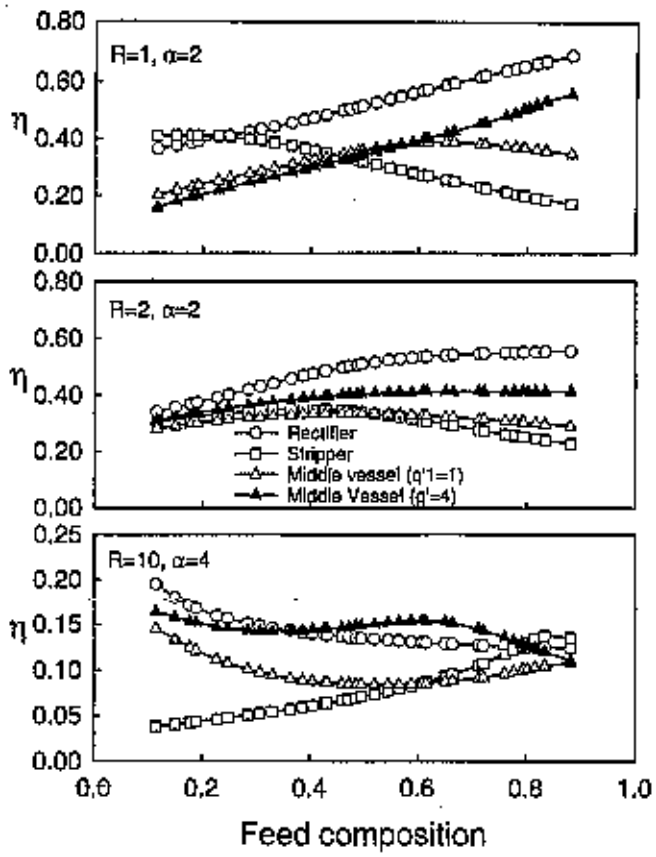

Figure 11. Comparison of thermodynamic efficiency for the rectifier, the stripper, and the middle-vessel column.

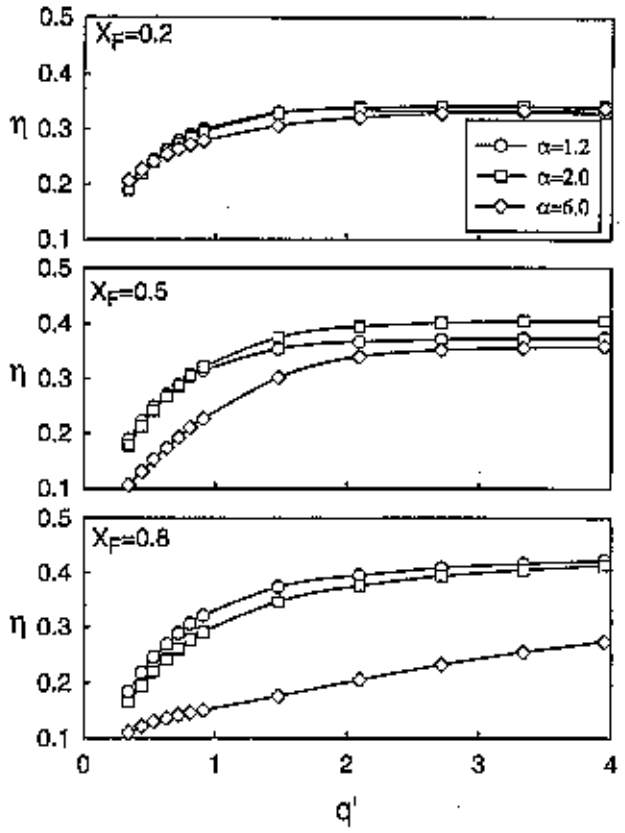

Figure 12. Effect of q' on the middle-vessel thermodynamic efficiency.

N and *R* are fixed to 5 and 2, respectively.

fier is also seen in this figure. In the top figure ($R=1$ and $\alpha=2$) the inversion in the stripper can be seen at low feed compositions, and the thermodynamic efficiency of the middle-vessel column with q' of 4 is still lower than that of the rectifier. In the middle figure ($R=2$ and $\alpha=2$), the rectifier still maintains higher thermodynamic efficiency. Lower thermodynamic efficiency of the stripper and the middle-vessel column indicate that heat exchange around these columns is not optimally configured and should be carried before their implementation in real problems. Adding an intermediate reboiler or an intermediate might be one option (Agrawal and Herron, 1998). The bottom figure ($R=10$ and $\alpha=4$) shows clear inversion in the stripper and the middle-vessel column. The inversion region of the stripper is restricted to the high feed composition region, while the inversion region of the middle-vessel column is relatively wide. Note that due to high R and α, the efficiencies of the three columns are low compared to the top the middle figures given earlier, and at these high-purity conditions the middle vessel η is higher. Figure 12 also shows the effect of q' on thermodynamic efficiency in terms of feed composition. As expected in Eq. 12, thermodynamic efficiency increases rapidly at low q' (usually lower than 3) in this figure, and then reaches a constant value.

In contrast to continuous distillation, the thermodynamic efficiency of batch column is relatively low at high product purity conditions. There are three main causes for this low efficiency. The first reason is that W_{min} in continuous distillation assumes pure products, and thus W_{min} is expressed only by the feed composition terms. However, in batch distillation, actual time-varying product compositions are used, and these additional terms reduce W_{min} and thus η. Second, the reboiler in the rectifier, the top still pot in the stripper, and the middle vessel are included in the exergy balance, and these reservoirs experience a large exergy change during batch process that results in a large exergy loss. If the bottom composition in the rectifier is less than 0.5, for example, the third term in Eq. 10 is positive, and thus W_{min} increases. However, small values in x_B also rapidly increase the denominator term

$$V \ln\left[\frac{x_{D,1}(\alpha-1)+1}{x_{B,1}(\alpha-1)+1}\right],$$

and hence thermodynamic efficiency is relatively small. For higher x_B (>0.5), the third term in W_{min} is negative and the resulting W_{min} decreases. Third, the thermodynamic efficiency used here is the averaged value because the thermodynamic efficiency equation is time dependent. The numerator in the efficiency equation represents the minimum work required to extract the desired product from the given feed, which is the current reboiler residue. In batch distillation the product purity and feed composition are varying in time and the increased composition difference will reduce the numerator term.

Table 2. Design Conditions for Each Case Number

Case No.	x_F	N	R	Case No.	x_F	N	R
1	0.2/0.8	14	10.0	6	0.2/0.8	9	7.75
2	0.2/0.8	13	9.10	7	0.2/0.8	8	7.30
3	0.2/0.8	12	9.10	8	0.2/0.8	7	6.85
4	0.2/0.8	11	8.65	9	0.2/0.8	6	6.40
5	0.2/0.8	10	8.20	10	0.2/0.8	5	5.95

Note: $\alpha = 2$; feed = 100 kmol.

Thermodynamic efficiency is an important performance index in this parametric study. It has several inversions in the stripper and in the middle-vessel column. When other performance indices, such as product purity and feasibility indices, cannot give the best solution, thermodynamic efficiency should be considered.

Case studies

In this article, we provided important performance indices (that is, objectives) for optimal batch column design, synthesis, and control, and behaviors of trade-offs between performance indices. This section presents some simple case studies for illustrating the usefulness of these indices. These studies present the first step toward the comprehensive framework for analyzing and quantifying objectives and design variables. To obtain the best alternatives, however, we will have to resort to a multiobjective optimization framework. Table 2 summarizes the design conditions used in these simple case studies. Under fixed α and feed amount, N and R are systematically changed for each low and high feed conditions. Figure 13 shows three performance indices; product purity, N-feasibility index, and thermodynamic efficiency, in accordance with different case numbers. R-Feasibility is omitted here because the reflux ratio can be optimally manipulated after column implementation. This figure is not intended to determine any details, but is intended to show the behavior of trade-offs among performance indices and the necessity of a multiobjective optimization framework.

In case number 1 in Figure 13a, the stripper has the highest product purity and the rectifier has the lowest product purity, but they are still high. However, the N-feasibility index and thermodynamic efficiency of the stripper are the lowest. Since the middle-vessel column at q' of 4 has high values in these three performances, this column configuration would be the best selection. On the other hand, in case number 10 in Figure 13a, the rectifier has the highest values in the three performance indices, and this column configuration can be chosen as an optimal column configuration. At high feed composition (Figure 13b), the stripper has high N-feasibility and thermodynamic efficiency in case number 1. However, the product purity of the stripper is quite low compared to other column configurations, and thus the stripper can be selected only if the product purity shown is acceptable. Otherwise, the middle-vessel column with q' of 4 would be the best choice. A situation like case number 10 is the most difficult one to decide. The product purity and thermodynamic efficiency of the rectifier are the highest, but N-feasibility is the lowest. This case can be optimized with more information about the sytem in a multiobjective optimization framework and shows difficulties of batch distillation synthesis. This multiobjective framework can identify the best designs for better profitability, flexibility, and operability, and will be the focus of our future work.

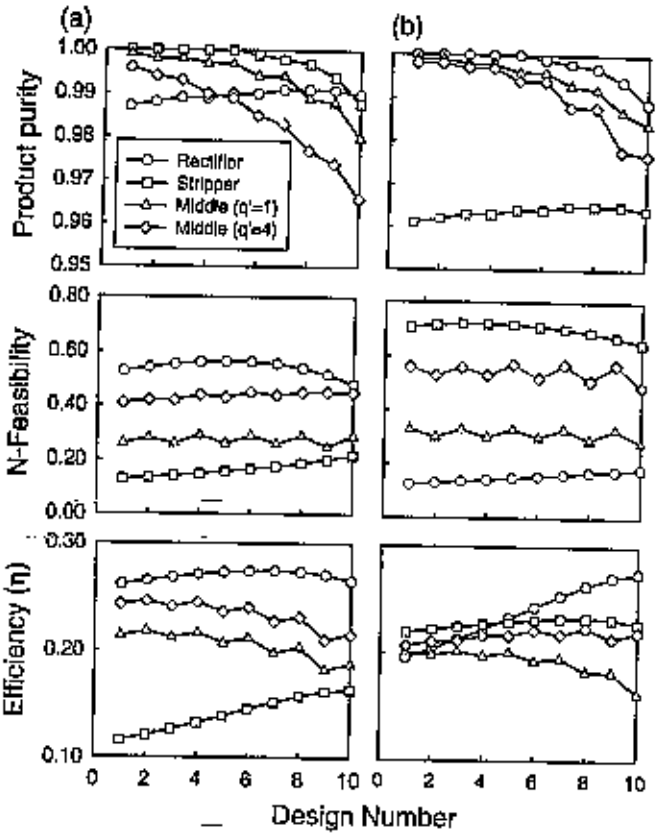

Figure 13. Trends of multiobjective functions with respect to case numbers.

(a) Feed composition = 0.2 (MVC); (b) feed composition = 0.2 (LVC).

Conclusions

Comparison of batch column configuration, including emerging designs such as the stripper and the middle-vessel column, is very important for batch distillation synthesis and establishes the potential usefulness of these columns. This study defined and analyzed various performance indices, such as product purity, feasibility indices, and thermodynamic efficiency, and obtained generalized heuristics for optimum column configuration. If the product purity of the MVC is a desired product, the rectifier is always a preferred column configuration, and this preference for the rectifier is enhanced as feed composition decreases. When the product purity index is combined with the N-feasibility index and thermodynamic efficiency, the use of the rectifier at low feed compositions is preferable. For the LVC product, it is concluded that the stripper is a better column configuration in terms of product purity and N-feasibility index, especially at high feed compositions. The middle-vessel column can provide high product purity for both the MVC and the LVC products simultaneously. For thermodynamic efficiency, it is generally observed that the rectifier has superior η to that of the stripper or the middle-vessel column. However, η inver-

sion can occur, especially when q' is varied. Because q' can significantly affect product purity, the N-feasibility index, and the thermodynamic efficiency of the middle-vessel column, the optimal value of q' should be chosen when the middle-vessel column is considered. Trade-offs between performance indices are also presented using simple case studies. This case study supports that the stripper or the middle-vessel column can be more flexible and operable than the rectifier at the same product purity. In order to obtain comprehensive heuristics for optimal batch column design and configuration, a multiobjective optimization technique is required to obtain higher profitability, flexibility, and operability. This task will be done with the help of coupled combinatorial and nonlinear programming optimization techniques and is the focus of a later article.

Acknowledgment

The authors thank the National Science Foundation and Mallinckrodt Chemicals for the funding of this research (CTS-972074). They also thank the two anonymous reviewers for providing valuable discussions and suggestions.

Notation

B = bottom residue (kmol) or bottom product flow rate, kmol/h
D = distillate, kmol/h
e = exergy, J/mol
h = enthalpy, J/mol
N = number of plates
N_B = number of bottom plates
q' = ratio of the top vapor flow rate to the bottom vapor flow rate
R = reflux ratio
R_B = reboil ratio
S = still pot residue, kmol
s = entropy, J/mol/K
T_o = reference (or environment) temperature, °C
T_C = condenser temperature, °C
T_R = reboiler temperature, °C
T_S = still pot temperature, °C
V, V_T = vapor rate in the rectifier or in the top section, kmol/h
V_B = vapor rate in the stripper or in the bottom section, kmol/h
W_{min} = minimum work of separation
x_B = bottom composition
x_D = distillate composition
x_N = liquid composition at tray N (from top)
x_S = still pot composition
y_B = vapor composition at the reboiler

Literature Cited

Agrawal, R., and D. M. Herron, "Optimal Thermodynamic Feed Conditions for Distillation of Ideal Binary Mixtures," *AIChE J.*, **43**, 2984 (1997).
Agrawal, R., and D. M. Herron, "Intermediate Reboiler and Condenser Arrangement for Binary Distillation Columns," *AIChE J.*, **44**, 823 (1998).
Agrawal, R., and Z. T. Fidkowski, "Are Thermally Coupled Distillation Columns Always Thermodynamically More Efficient for Ternary Distillations?" *Ind. Eng. Chem. Res.*, **37**, 3444 (1998).
Chiotti, O. J., and O. A. Iribarren, "Simplified Models for Binary Batch Distillation," *Comput. Chem. Eng.*, **15**, 1 (1991).
Davidyan, A., V. Kiva, G. Meski, and M. Morari, "Batch Distillation Column with a Middle Vessel," *Chem. Eng. Sci.*, **49**, 3033 (1994).
Diwekar, U. M., and K. P. Madhavan, "Multicomponent Batch Distillation Column Design," *Ind. Eng. Chem. Res.*, **30**, 713 (1991).
Diwekar, U. M., "Understanding Batch Distillation Process Principles with *MultiBatchDS*," *Chem. Eng. Educ.*, **4**, 275 (1996).
Diwekar, U. M., and J. R. Kalagnanam, "Efficiency Sampling Technique for Optimization under Uncertainty," *AIChE J.*, **43**, 440 (1997).
Fitzmorris, R. E., and R. S. H. Mah, "Improving Distillation Column Design Using Thermodynamic Availability Analysis," *AIChE J.*, **26**, 265 (1980).
Hasebe, S., A. Aziz, I. Hashimoto, and T. Watanabe, "Optimal Design and Operation of Complex Batch Distillation Column," *IFAC Workshop on Interaction Between Process Design and Process Control*, p. 177 (1992).
Hasebe, S., M. Noda, and I. Hashimoto, "Optimal Operation Policy for Multi-Effect Batch Distillation System," *Comput. Chem. Eng.*, **21**, S1221 (1997).
Lotter, S. P., and U. M. Diwekar, "Shortcut Models and Feasibility Considerations for Emerging Batch Distillation Columns," *Ind. Eng. Chem. Res.*, **36**, 760 (1997).
Meski, G. A., and M. Morari, "Design and Operation of a Batch Distillation," *Comput. Chem. Eng.*, **19**, S597 (1995).
Muftaba, I. M., and S. Macchietto, "Optimal Operation of Multicomponent Batch Distillation. A Comparative Study Using Conventional and Conventional Columns," *Proc. ADCHEM '94*, Japan (1994).
Robinson, C. S., and E. R. Gilliland, *Elements of Fractional Distillation*, 4th ed., McGraw-Hill, New York (1950).
Safrit, B. T., A. W. Westerberg, U. M. Diwekar, and O. M. Wahnschafft, "Extending Continuous Conventional and Extraction Distillation Feasibility Insights to Batch Distillation," *Ind. Eng. Chem. Res.*, **34**, 3257 (1995).
Skogestad, S., B. Wittens, R. Litto, and E. Sørensen, "Multivessel Batch Distillation," *AIChE J.*, **43**, 971 (1997).
Sørensen, E., and S. Skogestad, "Comparison of Regular and Inverted Batch Distillation," *Chem. Eng. Sci.*, **51**, 4949 (1996).
Swaney, R. E., and I. E. Grossmann, "An Index for Operational Flexibility in Chemical Process Design: 1. Formulation and Theory," *AIChE J.*, **31**, 621 (1985).

Appendix: Derivation of Thermodynamic Efficiency

Figure 2 shows the system boundary for the exergy balance. As described earlier, the reservoirs in the three batch column configurations are included in the system boundary due to large exergy changes inside the reservoirs. The exergy balance for the rectifier is given by

$$\frac{d}{dt}(B\epsilon_B) = Le_L - V\epsilon_V + \left(1-\frac{T_o}{T_R}\right)Q_R - \epsilon_{loss}. \quad (A1)$$

The term on the lefthand side, $d/dt(B\epsilon_B)$, represents exergy change in the reboiler. The first two terms on the righthand side show exergy flows around the column. The third term defines the exergy input to the reboiler, and the last term shows exergy loss (ϵ_{loss}) due to process irreversibility of the column internals, concentration, and temperaure changes.

In general, exergy comprises physical (ϵ_{ph}) and chemical (ϵ_{ch}) components. Physical exergy comes from physical processes involving thermal interaction with the surroundings, while chemical exergy accounts for heat and mass transfer with the surroundings. Mixing effects, the major one in the chemical exergy components can be estimated by chemical potential at low pressure, which can result in $RT_o\Sigma x_i \ln x_i$. Chemical reactions are not considered here, and the reference state is the liquid state at 25°C and 1 atm. Then the exergies of the liquid stream (L), vapor stream (V), and the

reboiler (B) can be defined as

$$\epsilon_L = \epsilon_{ph,L} + RT_o\Sigma x_{D,i}\ln x_{D,i} \quad \text{(A2)}$$

$$\epsilon_V = \epsilon_{ph,V} + \Delta H_{vap}\left(1-\frac{T_o}{T_C}\right) + RT_o\Sigma x_{D,i}\ln x_{D,i} \quad \text{(A3)}$$

$$\epsilon_B = \epsilon_{ph,B} + RT_o\Sigma x_{B,i}\ln x_{B,i}. \quad \text{(A4)}$$

Physical exergy can be assumed to be constant for all chemical species because this term is relatively smaller than its chemical component. Thus the constant physical exergy terms will be canceled out during derivation. Note that constant molar overflow is assumed in the batch-distillation model. The final assumption inserted here is the same heat of vaporization for each component, and heat of vaporization is independent of temperature. The exergy change in the reboiler can be extended as follows:

$$\frac{d}{dt}(B\epsilon_B) = \epsilon_B\frac{dB}{dt} + B\frac{d\epsilon_B}{dt}$$
$$= -D(\epsilon_{ph,B} + RT_o\Sigma x_{B,i}\ln x_{B,i}) + BRT_o\frac{d}{dt}(\Sigma x_{B,i}\ln x_{B,i}). \quad \text{(A5)}$$

The derivative in the last term can be treated as a difference equation between the current and previous time steps for computational convenience.

Reboiler heat duty (Q_R) can be estimated by the energy balance, and the resulting equation becomes

$$Q_R = V\Delta H_{vap}. \quad \text{(A6)}$$

Using the preceding equations, the first three terms in the righthand side of Eq. A1 become:

$$L\epsilon_L - V\epsilon_V + \left(1-\frac{T_o}{T_R}\right)Q_R$$
$$= (L\epsilon_{ph,L} - V\epsilon_{ph,V}) + V\Delta H_{vap}T_o\left(\frac{1}{T_C}-\frac{1}{T_R}\right) - DRT_o\Sigma x_{D,i}\ln x_{D,i}$$
$$= (L\epsilon_{ph,L} - V\epsilon_{ph,V}) + VRT_o\ln\left[\frac{x_{D,1}(\alpha-1)+1}{x_{B,1}(\alpha-1)+1}\right] - DRT_o\Sigma x_{D,i}\ln x_{D,i}. \quad \text{(A7)}$$

In the preceding derivation, the condenser and reboiler temperatures (T_C and T_R) are eliminated with the help of the Clausius-Claypeyron equation,

$$\ln\frac{P}{P_{vap,A}} = \frac{\Delta H_{vap}}{R}\left(\frac{1}{T}-\frac{1}{T_A}\right),$$

where T_A is the boiling point of the more volatile component A (or 1). Then the exergy loss can be derived, and it always should be positive:

$$\epsilon_{loss} = L\epsilon_L - V\epsilon_V + \left(1-\frac{T_o}{T_R}\right)Q_R - \frac{d}{dt}(B\epsilon_B) > 0$$
$$= -DRT_o\Sigma x_{D,i}\ln x_{D,i} + DRT_o\Sigma x_{B,i}\ln x_{B,i} - BRT_o\frac{d}{dt}(\Sigma x_{B,i}\ln x_{B,i}) + VRT_o\ln\left[\frac{x_{D,1}(\alpha-1)+1}{x_{B,1}(\alpha-1)+1}\right] \quad \text{(A8)}$$
$$= -W_{min} + VRT_o\ln\left[\frac{x_{D,1}(\alpha-1)+1}{x_{B,1}(\alpha-1)+1}\right]. \quad \text{(A9)}$$

Physical exergy terms are canceled out during this derivation. The W_{min} can be defined as the chemical exergy difference between the intermediate product and the reboiler residue. Finally, the thermodynamic efficiency of the rectifier is defined as follows:

$$\eta_{rectifier} = \frac{W_{min}}{W_{min}+\epsilon_{loss}} = \frac{W_{min}}{V\ln\left[\frac{x_{D,1}(\alpha-1)+1}{x_{B,1}(\alpha-1)+1}\right]}, \quad \text{(A10)}$$

where

$$W_{min} = D\Sigma x_{D,i}\ln x_{D,i} - D\Sigma x_{B,i}\ln x_{B,i} + B\frac{d}{dt}(\Sigma x_{B,i}\ln x_{B,i}). \quad \text{(A11)}$$

The thermodynamic efficiency of the rectifier is a function of the vapor flow rate, distillate flow, amount in the reservoir, reboiler and condenser compositions, and relative volatility. But this is not an explicit function of the reboiler and condenser temperatures. Note also that the reference temperature T_o is also canceled out during derivation. This equation is similar to the one for continuous distillation (Agrawal and Herron, 1997), but the W_{min} of batch distillation is more complex due to the time-depending nature. Using the same derivation procedure, thermodynamic efficiencies of the stripper and the middle vessel are:

For the stripper,

$$\eta_{stripper} = \frac{W_{min}}{V_B\ln\left[\frac{x_{S,1}(\alpha-1)+1}{x_{B,1}(\alpha-1)+1}\right]}, \quad \text{(A12)}$$

where

$$W_{min} = -V_B \Sigma y_{B,i} \ln y_{B,i} + L_B \Sigma x_{N,i} \ln x_{N,i} - \left(\frac{dB}{dt}\right) \Sigma x_{S,i} \ln x_{S,i} + S \frac{d}{dt} (\Sigma x_{S,i} \ln x_{S,i}); \quad \text{(A13)}$$

For the middle-vessel column,

$$\eta_{middle} = \frac{W_{min}}{q' V_B \ln \left[\frac{XD_1(\alpha - 1) + 1}{XS_1(\alpha - 1) + 1}\right] + V_B \ln \left[\frac{XS_1(\alpha - 1) + 1}{XB_1(\alpha - 1) + 1}\right]}, \quad \text{(A14)}$$

where

$$W_{min} = D \Sigma x_{D,i} \ln x_{D,i} - V_B \Sigma y_{B,i} \ln y_{B,i} - L_B \Sigma x_{N,i} \ln x_{N,i} + \left(\frac{dS}{dt}\right) \Sigma x_{S,i} \ln x_{S,i} + S \frac{d}{dt} (\Sigma x_{S,i} \ln x_{S,i}). \quad \text{(A15)}$$

For the stripper and the middle-vessel column, the W_{min} requires y_R and x_N, which represent the vapor and liquid stream compositions around the reboiler. The thermodynamic efficiency of the middle-vessel column has another variable that is the ratio of the top and bottom vapor flow rates (q'). This variable can provide flexibility to the middle-vessel column and can manipulate the thermodynamic efficiency at the same product purity. Batch distillation is such a transient process, in that its thermodynamic efficiency is also time dependent—unlike that of continuous distillation. In this article, average values of thermodynamic efficiency are used to compare efficiency caused by different column configurations.

Manuscript received Nov. 19, 1999, and revision received June 7, 2000.